

NEW CLUES FROM THE MICROSTRUCTURE OF JUPITER'S S-BURSTS

T. D. Carr*

Abstract

Until recent years essentially all the information regarding Jupiter's decametric narrow-band frequency-drifting S-bursts had been acquired by means of radio telescope dynamic spectrographs having resolutions no finer than 300 μ s in time and 3 kHz in frequency. Such limited information alone is inadequate to serve as a basis for the formulation of a realistic emission model. With the development by Carr and Reyes [1999] of a method for obtaining information from S-bursts with time resolutions of about 3 μ s and 0.3 kHz together with the use of a radio telescope antenna of very large collecting area, however, a window was opened on a rich new source of detailed information that is closely connected with the source mechanism. Further improvements made in the data analysis techniques since the publication of the Carr and Reyes paper are described here, followed by the presentation of some interesting new results obtained from a re-analysis of old data. Phase coherent intervals were found to be much more widely distributed within an S-burst than we had previously thought. An elevated background noise level, suggested to be amplified galactic radiation, was observed immediately before the occurrence of an S-burst; its intensity level dropped immediately after the decay of the S-burst intensity at each frequency. Phase jumps of 180° observed during intervals of phase coherence are tentatively suggested to be indicative of intermittent phase lock via second-harmonic radiation exchanged between a pair of centers of cyclotron maser amplification, the fundamental frequency component from one of which is beamed toward Earth.

1 Background

Most of the Jovian decametric emission observed from Earth is in the form of sporadic bursts. The most common type is the L-burst. The durations of L-bursts vary between about 2 and 10 s. A typical L-burst observed at a frequency in the vicinity of 20 MHz is electromagnetic noise with a Gaussian amplitude distribution that is limited to a bandwidth of 2 MHz or so, its modulation envelope being in the form of a smoothly rising and

**Department of Astronomy, University of Florida, Gainesville, Florida 32611, USA*

falling curve. L-burst dynamic spectra have no repeatable structural detail at frequencies higher than the components impressed by interplanetary scintillation, which are less than 1 Hz. Individual S-bursts, on the other hand, are of much shorter duration and narrower bandwidth, and may have highly complex dynamic spectra. An S-burst is identified by the presence of a relatively strong spectral component consisting of an intense, narrow, downward-drifting frequency band. The frequency-drifting bandwidth of this component is usually in the vicinity of 20 kHz, and the drift rate is usually between 5 and 40 MHz/s. Much wider-band components may also be present in complex S-bursts. S-bursts are usually repetitive, with repetition rates most often being between about 10 and 100 per second. S-bursts usually occur over relatively brief intervals of intense activity within Io-controlled Jovian storms consisting otherwise of L-bursts.

Until 1997 nearly all of the available information on the nature of Jovian S-bursts was derived from dynamic spectral observations for which the best obtainable resolution was about 0.3 millisecond in time and 3 kHz in frequency. The phenomenology based on such observations is well documented (see the extensive reference list in Carr and Reyes [1999]). There is a great deal of evidence to support the long-standing assumption that both the L-bursts and S-bursts are emitted in the X-mode of propagation at frequencies slightly higher than the local electron cyclotron frequency, f_c . In the case of the Io-controlled emissions the source is located near the foot of a tube of Jovian magnetic flux which has been disturbed by its passage across the Jovian satellite Io as the flux tube corotates with the planet. This disturbance presumably propagates down the Io-excited flux tube in the form of Alfvén waves (although this assumption has not yet been proven correct) to the radio source location, where it somehow initiates the radio emission. The emission is beamed within a thin curved sheet in the form of an azimuthal sector of a cone making an angle of about 70° with the magnetic field line through the source. A condition for such radiation to be observable from earth is that the source is being excited at a time at which the thin-curved-sheet beam is suitably oriented earthward.

Despite the similarity in the frequencies and beaming patterns of L and S-bursts, certain aspects of their emission mechanisms must be very different. For example, the narrow instantaneous bandwidth of S-bursts, their downward frequency drift, and other characteristics strongly suggest that the source is relatively small (probably on the order of 1 or 10 km) and that the group of magnetically trapped gyrating electrons of which it is composed is traveling upward along the Io flux tube with a velocity component v_{\parallel} (tangent to the magnetic field lines) on the order of 20000 km/s (see the discussion of Figure 1 below). The L-burst sources, on the other hand, probably consist of gyrating electrons that are much more widely dispersed than are those of S-bursts, and apparently do not possess relatively high parallel velocity components that would lead to observable frequency drifts.

Following the discovery of radio noise emissions from the magnetosphere of Earth that are of considerably lower frequency than is Jupiter's decametric radiation (referred to as the auroral kilometric radiation, or AKR), the cyclotron maser emission model was proposed by Wu and Lee [1979]. This model, with subsequent additions, has proved eminently successful. Although it is now generally assumed that variants of the Wu and Lee cyclotron maser model can probably be developed that will also account for the Jovian

decametric emissions, this has not yet been accomplished. More information regarding the nature of the Jovian magnetosphere in the vicinity of the radio source locations will probably be required before a successful model can be constructed for any of its low frequency radio emissions.

In the cyclotron maser a seed wave, usually assumed to be galactic background noise, is amplified by a stream of mildly relativistic magnetically trapped electrons possessing an unstable loss-cone pitch angle distribution. This instability is the result of a recent mirroring of the electrons. Those with relatively small pitch angles collided with neutral atoms before reaching their mirror points, resulting in their precipitation into the lower atmosphere. The pitch angle distribution of the electrons remaining after mirroring is unstable because of the deficiency in the relative numbers with small pitch angles (and low gyration energies), corresponding to an excess of those with large pitch angles (and high gyration energies) in comparison with the case of a stable distribution. When a stream of electrons having such an unstable distribution happen under suitable conditions to interact with an electromagnetic wave of frequency close to their f_c value, the mean energy transferred from the electrons to the wave will be greater than that from the wave to the electrons. The result is the amplification of the wave. If the electron population regained a stable pitch angle distribution, the wave-to-electron and electron-to-wave energy transfers would become equal and there would no longer be wave amplification.

Since the transfers of excess energy from the electrons to the wave occur at random times due to the random spatial distribution of the electrons, the wave amplification by the cyclotron maser is phase incoherent. The oscillation frequency of the electromagnetic field vector $\mathbf{E}(t)$ never remains constant. It drifts relatively slowly back and forth within the bandwidth. The radiation is narrow-band radio noise. By narrow-band it is meant that $\Delta f \ll f_1$, where Δf is the bandwidth and f_1 is the lowest frequency within the band. The mean time between successive reversals of the frequency drift direction is of the same order of magnitude as the reciprocal of the bandwidth. Similarly the amplitude of the envelope of the oscillations of $\mathbf{E}(t)$ is continually fluctuating, the mean times between successive fluctuation peaks being similarly related to the reciprocal of the bandwidth.

Melrose [1986a] indicates that for a population of electrons having an unstable pitch angle distribution to be able to amplify an electromagnetic wave *coherently* there would have to be some *phase-bunching* feedback mechanism, one that would maintain the orderly arrangement of the phases of the individual gyrating electrons that are about to deliver energy to the wave. The bandwidth of the amplified wave would in such a case be very narrow, ideally approaching zero, and the radiation would be nearly sinusoidal (but with harmonics if the relativistic mass increase with electron velocity is not negligible). The best-known naturally occurring mechanism in which such a process takes place is that producing *whistlers* in Earth's magnetosphere. In the whistler emission mechanism there is a continual feedback of already-amplified radiation in such a way as to maintain the phase bunching of those electrons that are about to participate in the continuation of the amplification process. Melrose, assuming the phase coherence of Jovian S-bursts, suggested that S-burst emission might involve the exchange of radiation between two centers of activity within a cyclotron maser in such a way as to produce synchronized phase bunching of the gyrating energetic electrons at the two locations. Calvert et al.

[1988] had previously suggested that the feedback required to maintain phase coherence is provided by the mirroring of emitted radiation back to the oscillator in some unspecified way. It is most unlikely, however, that the high plasma density that would be required to produce such a reflection (or extreme degree of refraction) ever exists in the vicinity of S-burst sources.

2 Previous observations of the S-burst microstructure

Previous observations of S-burst microstructure, that is, of the structure of time and frequency variations as revealed at a resolution much finer than 0.3 ms in time and 3 kHz in frequency, appear in only four publications, so far as I am aware. The first two, by Flagg and Carr [1967] and Trapp [1971] were crude but provided evidence of the existence of important spectral information that could be properly extracted only by the use of a much finer degree of resolution and a much more sensitive receiving system than was available at that time. The other two of the publications were those of Carr et al. [1997] and Carr and Reyes [1999]. I will henceforth refer to the latter as Paper 1. The 1997 paper contains a preliminary report on the results subsequently presented in Paper 1. Paper 1 also contains brief accounts of the early results of Flagg and Carr [1967] and of Trapp [1971].

Our results presented in Paper 1 were obtained from S-burst data stored in the University of Florida Radio Observatory archives. The observations had been made with the use of the 640-dipole antenna array. This large antenna had a half-power bandwidth of somewhat more than 1 MHz, with a center frequency of 26.3 MHz. Receivers of different bandwidths were used at different times, their bandwidth range being from 150 kHz to 1 MHz. The baseband output of the receiver in use was analog tape recorded at a tape speed of 120 inches/s. When the system was originally being used for obtaining dynamic spectra of Jovian S-bursts, it was entirely analog. On playback the tape speed was reduced by a factor of 1/128. This time-expanded played-back analog signal was delivered to an audio-frequency spectrum analyzer which repeatedly calculated signal intensity as a function of frequency and time, finally providing the dynamic spectrum in the familiar format that was used for many years (examples can be seen in Figure 1). A modification of the old all-analog system by Francisco Reyes now makes it possible to digitize the previously recorded analog data as it is played back at the tape speed reduction factor of 1/128, yielding digital data having a real-time equivalent sampling period of 0.3125 μ s. It is this high sampling rate that has made possible our S-burst microstructure investigations.

We have limited our study thus far to the simplest form of S-bursts, similar to those illustrated in Figure 1. When displayed with a resolution of 0.3 ms and 3 kHz their dynamic spectra appear as sloping lines with negligible curvature, broadening, or branching. Although such simple linear-drift S-bursts are not common, we have decided not to complicate the situation by trying to explain the intricacies of complex S-bursts before an understanding of the origin of the simple ones is reached. I will first mention some preliminary results of measurements at this relatively low resolution that were presented in Paper 1 before proceeding with the discussion of those made at the highest

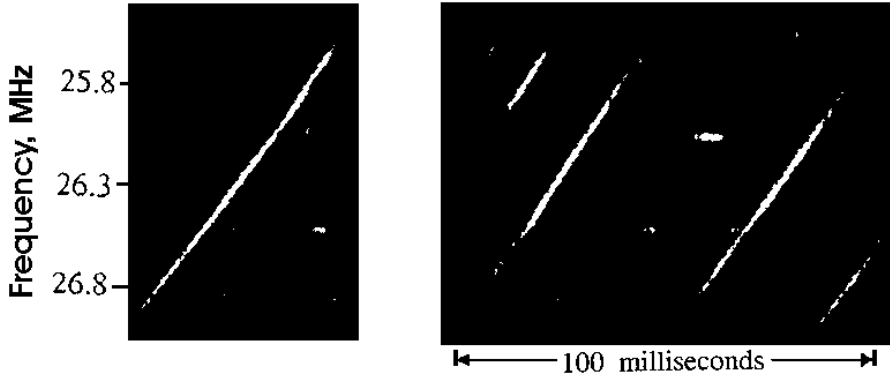


Figure 1: Dynamic spectra of simple linear-drift S-bursts. Recorded at the University of Florida Radio Observatory during an Io-A storm at about 01:44 UT on December 26, 1988; the 640-dipole antenna array was used (from Flagg et al. [1991]).

resolution. Using an enlarged image of the S-burst at the extreme left in Figure 1, we made a straight-line fit to its median line and measured its slope, (df/dt) . It was -29.3 ± 0.4 MHz/s. The source location and the field gradient dB/ds at the source were estimated from the time, frequency, central meridian longitude, and Io orbital phase, together with the O6 magnetic field model. Assuming that f and f_c are equal, we calculated the parallel velocity component of the source in its outward motion along the Io flux tube from the relation

$$v_{\parallel} = \frac{(df_c/dt)}{(df_c/ds)} \quad (1)$$

The value of v_{\parallel} was found to be 24.600 ± 500 km/s. A search for a change in the frequency-drift slope between the first and second halves of the S-burst revealed that there was none exceeding the measurement error limits. These measurements together with supplementary information obtained from another S-burst enabled us to estimate the electron energy $\frac{1}{2}m(v_{\perp}^2 + v_{\parallel}^2)$. It was found to be 7 ± 3 keV. A similar value was found by Zarka et al. [1996] by a very different method. The fact that these values are in agreement with the energies of the electrons involved in the emission of terrestrial AKR, about 5 keV, is consistent with the assumption that the cyclotron maser is involved in the emission of Jovian S-bursts. The fact that we could detect no change in the slope of an S-burst of the type selected for our measurements also suggests that the emitting electrons were not subject to an acceleration by an appreciable parallel electric field component E_{\parallel} , since dv_{\parallel}/dt was zero in the force equation $eE_{\parallel} = mdv_{\parallel}/dt$. The elimination of the need to consider an E_{\parallel} component presumably simplifies the task of developing an emission model.

I now return to the discussion of the high-resolution data analysis procedures and results on which we reported in Paper 1. Our most important results of this type were undoubtedly the discoveries in the fine structure of simple S-bursts of a) deep envelope

fluctuations and b) intervals of phase coherence. The envelope fluctuations are usually well separated, and are not unlike those that are inherent in narrow-band phase incoherent noise. We found their most probable period to be about 90 μs . Such a fluctuation period would suggest a bandwidth of about 10 kHz if the noise is phase incoherent. With regard to the observed intervals of phase coherence, we demonstrated in Paper 1 that the most powerful subpulse in the entire S-burst that we investigated with high resolution was almost entirely phase coherent (after the smoothing indicated in equation (2) below had largely removed effects of higher frequency noise components).

I present here a brief explanation of the method that we developed to detect intervals of phase coherence. Let $v(t)$ be the S-burst voltage at the baseband output terminals of the receiver. We compare with $v(t)$ the signal voltage from a hypothetical matching oscillator, which is of the form $v_m(t) = \cos(2\pi f_m t + \delta_m)$. The frequency f_m and phase constant δ_m are adjustable parameters that are systematically varied in the search for the best match over a given time segment. The appropriately smoothed time variation of the cross correlation coefficient of $v_m(t)$ with $v(t)$ is given by

$$C(f_m, \delta_m, t) = \frac{\langle vv_m \rangle}{(\langle v^2 \rangle \langle v_m^2 \rangle)^{\frac{1}{2}}} = \frac{\langle vv_m \rangle}{(2 \langle v^2 \rangle)^{\frac{1}{2}}} \quad (2)$$

The brackets indicate running averages, which in Paper 1 were obtained by 10-point boxcar smoothing (the points being 0.3125 μs apart). An interval of phase coherence is revealed by finding a particular pair of the values f_m and δ_m that will cause the curve $C(f_m, \delta_m, t)$ versus t to become the straight line $C = 1$ over the interval.

In the investigation reported in Paper 1 we also used a second method for indicating intervals of phase coherence. In it the resultant phase difference between $v(t)$ and $v_m(t)$ was calculated as a function of time after a preliminary optimization of the parameters f_m, δ_m by means of the correlation coefficient method had been made. At in-phase resonance, $\varphi(t) = 0$. The measurement precision of $\varphi(t)$ during an interval of phase coherence was found to be about $\pm 5^\circ$. Although this second method provided an increase in precision, it is much more tedious to use than is the first method alone.

3 Improvements in technique, new results, and suggested interpretations

Since Paper 1 appeared, I have improved the data analysis procedures for the investigation of S-burst microstructure. The greatest improvements in this regard have resulted from the use of Matlab software, with its supplementary Signal Processing Toolbox. This software is well suited for efficiently performing the required calculations and for plotting. I report here on the following improvements: a) Use of Matlab software for making contour plots of S-burst dynamic spectra. b) Improvement of the method for systematically calculating and plotting the correlation coefficient function, $C(f_m, \delta_m, t)$ versus t , for assumed values of the adjustable parameters f_m and δ_m . c) Application of the correlation coefficient method to a synthesized sample of narrow-band noise, known to be completely

phase incoherent, in order to gain experience in distinguishing between phase incoherent and partially phase coherent intervals within an S-burst. When I tested these improvements on the same linear-drift S-burst that was used for the microstructure study in Paper 1, some important new results were obtained. These results are presented in the remainder of this paper, along with some interpretations that I tentatively offer.

In Figure 2, contours of constant radiation intensity are plotted as a function of frequency and time for a relatively weak S-burst that immediately preceded the one shown in Figure 3 of Paper 1. This plot was made from the digitized S-burst voltage data, $v(t)$, by means of a Matlab plotting function. The plotting sensitivity employed for Figure 2a was made relatively low in order to reveal the most intense region, where the contours are so close together that they become the black area near $t = 7$ ms, $f = 280$ kHz. The time resolution of the contour plots is insufficient to reveal individual subpulses. In Figure 2b, the plotting sensitivity has been increased by a factor of 100 to a point at which the galactic background can be clearly seen. The fact that the galactic noise appears only within a frequency band extending from about 180 to 320 kHz (at the receiver baseband output terminals) is due to the use of an RF bandpass filter inserted between the antenna output and the receiver input that admitted mainly the frequency components in the range 26.13 to 26.27 MHz. (Such a narrow filter was used on only this one occasion). The presence of the filter fortunately provides proof that the background noise contours seen here are indeed of galactic origin instead of being receiver noise. Since the receiver itself was of considerably wider bandwidth than was the bandpass filter; the band of receiver noise would easily have been identifiable here.

Figures 2b and 2c reveal a previously unobserved phenomenon. It is apparent that in these plots the background noise intensity is less after the S-burst occurrence at each frequency than it was before. One interpretation is that a particularly high density of free energy within the region in which the S-burst is about to form provides a certain amount of preliminary amplification of the galactic radiation within a narrow frequency band centered of the local value of f_c at each location before the onset of the S-burst. This preamplified galactic radiation provides the seed waves required for the initiation of the S-burst and for the restarting of it after each of the series of shut-downs that occur during its lifetime. The amplification of the growing S-burst at the successively lower f_c values occurs at the expense of the available free energy, which becomes depleted as a result. By the time the S-burst oscillation has decayed in intensity at each of its frequencies there is little or no free energy left for galactic amplification at that frequency. This is the reason for the observed drop in background level at the upper right of the S-burst in Figure 2c.

I will now describe the brief investigation to evaluate the effectiveness of my improved Matlab $C(f_m, \delta_m, t)$ algorithm for distinguishing between intervals of partially phase-coherent and completely phase-incoherent S-burst noise. As indicated previously, f_m and δ_m represent the frequency and phase constant of the virtual matching oscillator that is used to search for intervals of resonance with the S-burst. Such an interval can be recognized by the occurrence of a "zero beat" relationship between the S-burst and the matching oscillator. When f_m is adjusted for zero beat, $C(f_m, \delta_m, t)$ becomes constant, and this constant can be made to have the value 1.0 by adjustment of δ_m . The zero-beat

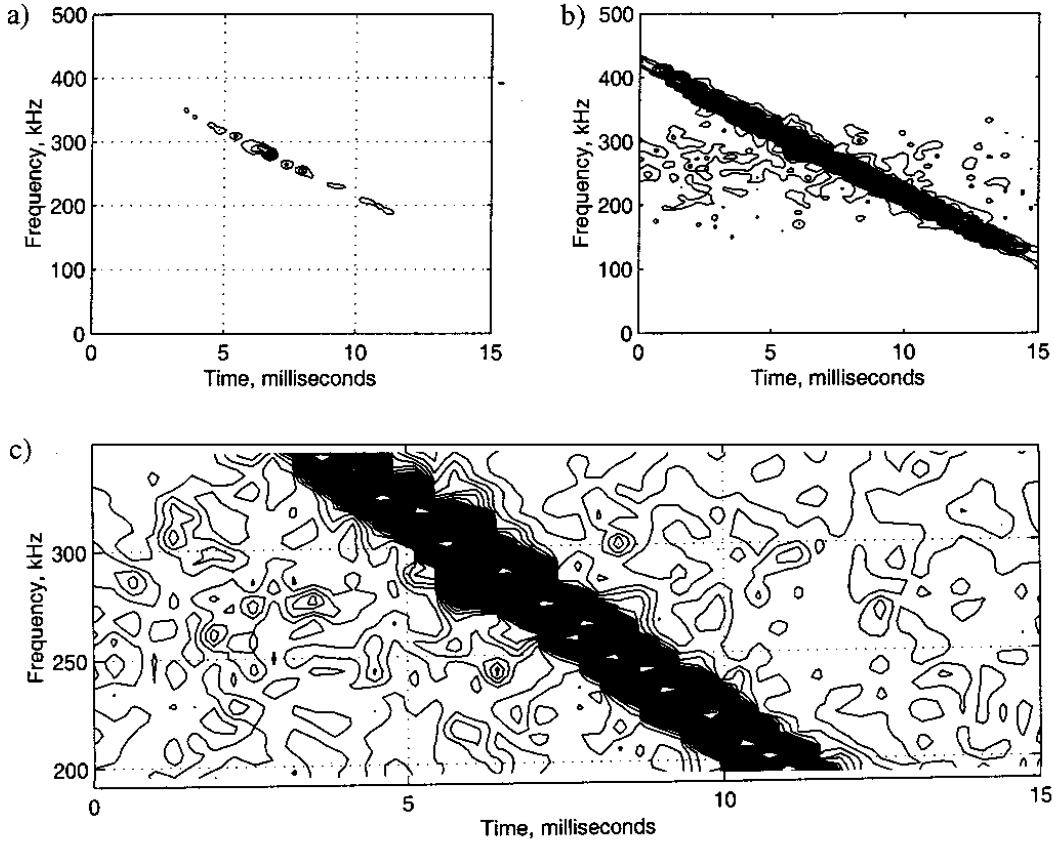


Figure 2: Dynamic spectrum of another S-burst displayed as iso-power density contours of the receiver baseband output signal plotted as a function of frequency and time. Observed during an Io-A storm at about 08:01 UT on November 12, 1977. Observing conditions were the same as for the S-burst in Figure 1 except that there was a bandpass filter between the antenna output and the receiver input in this case. a) With low plotting sensitivity. b) With plotting sensitivity increased by a factor of 100. Note the presence of galactic background radiation. c) With plotting sensitivity further increased by a factor of 2. It should be noted that the background noise intensity after the occurrence of the S-burst has been considerably reduced relative to that preceding it.

condition persists only as long as the S-burst remains phase coherent. It should be noted here that during such zero-beat intervals it is only the lowest frequency components of the S-burst that are phase coherent. The higher frequency components, which are removed by low-pass filtering, have not yet been investigated. In my improved algorithm for the correlation coefficient versus time, the low-pass filtering (indicated by the averaging brackets in equation (2)) is accomplished by separately convolving the numerator and the denominator of the expression with an 8-point Hanning window, the point separation being $0.3125 \mu\text{s}$.

In Paper 1 we had assumed that the criterion for judging a given S-burst interval to be completely phase incoherent is that there is no pair of the values f_m , δ_m for which the function $C(f_m, \delta_m, t)$ dwells at the line $C = 1$ for an appreciable length of time, despite the fact that its peaks are often tangent to the line. In order to reassure myself that this is correct and to gain experience in distinguishing between intervals of phase incoherent

and partially phase coherent narrow-band noise, I tested the algorithm for $C(f_m, \delta_m, t)$ on a synthesized 1-ms interval of narrow-band noise voltage $v(t)$ that was known to be completely phase incoherent. The sample is shown in Figure 3a.

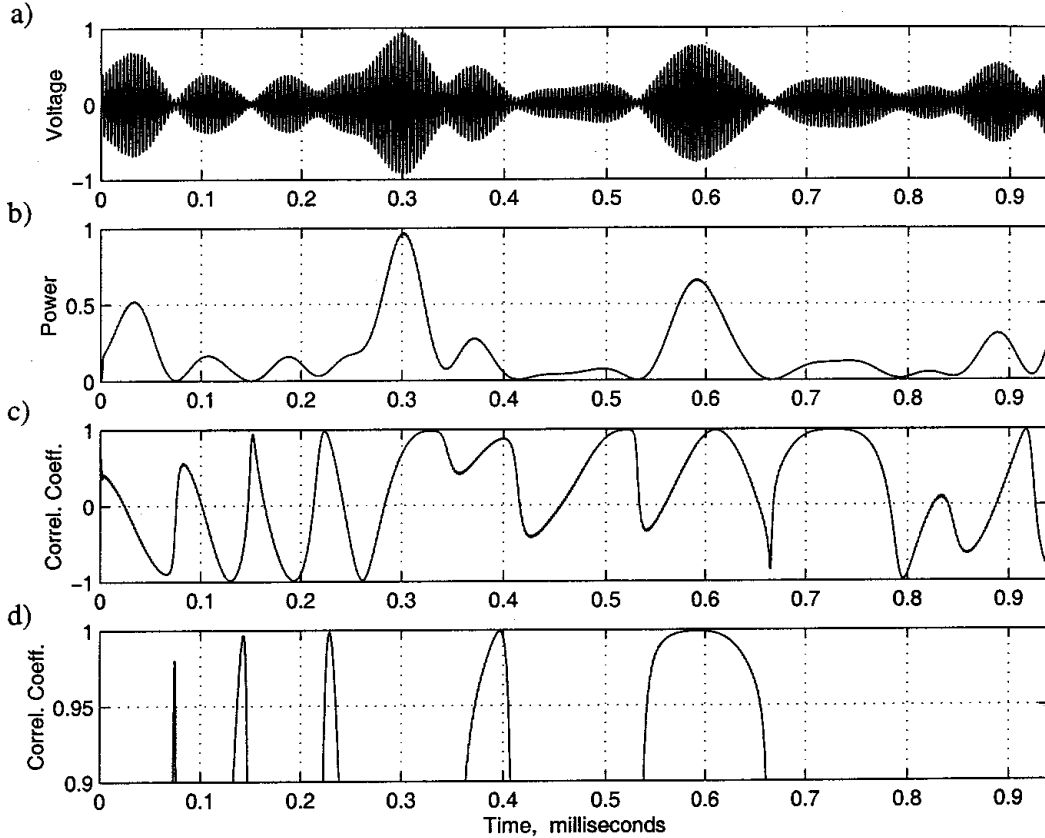


Figure 3: a) Voltage versus time plot of synthesized phase incoherent noise of 285 kHz center frequency and 20 kHz bandwidth. b) The same except that power (somewhat smoothed) is plotted versus time. c) Correlation coefficient of the noise voltage with that of the matching oscillator when the latter is set to the frequency 280 kHz and phase constant 140° . d) The same except that the matching oscillator is set to the frequency 285 kHz and phase constant 120° .

It was produced by the superposition of 200 sinusoidal components having closely and equally spaced frequencies from 275 to 295 kHz, their respective phase constants consisting of random numbers between 0 and 2π . The bandwidth of the noise (neglecting end effects) is 20 kHz. Figure 3b gives the curve of smoothed power corresponding to the voltage curve. Figures 3c and 3d show the wandering curve of the correlation coefficient $C(f_m, \delta_m, t)$, for randomly chosen pairs of the values f_m and δ_m , plotted versus t . These two curves and many others that I have examined illustrate the correctness of my previous assumption that for completely incoherent noise the curve often touches the lines $C = 1$ or $C = -1$ but never dwells at either place. On the other hand, if an interval of S-burst noise is found for which the curve $C(f_m, \delta_m, t)$ versus t remains at the value 1.0 for an interval Δt when a particular pair of the parameters f_m and δ_m have been assumed, then it must

Table 1: Observed phase coherent intervals

t_1	t_2	f	δ	C range	Δt
ms	ms	kHz	°		μs
6.15	6.20	295	68	0.95 to 1.00	45
6.28	6.36	286	285	0.93 to 1.00	75
6.28	6.37	285	44	0.94 to 1.00	90
6.37	6.39	293	55	0.96 to 1.00	25
6.41	6.49				78
6.47	6.58	289	25	0.96 to 1.00	115
6.72	6.79	286	242	0.97 to 1.00	69
6.72	6.80	285	157	0.97 to 1.00	84
6.78	6.85	281	210	0.97 to 1.00	70
6.82	6.91	279	90	0.98 to 1.00	87

have been phase coherent for that interval. Examples of such phase coherent intervals can be seen in Figure 4.

Figure 4 contains 12 plots of the correlation coefficient $C(f_m, \delta_m, t)$ for the baseband receiver and virtual matching oscillator outputs over a 1200 μs segment of the same S-burst that is shown in Figure 3 of Paper 1. Each of the curves resulted from the use of a pair of the settings f_m and δ_m of the matching oscillator that had been optimized to best display an interval of phase coherence in which $C = 1.0$. Many pairs of the parameters were used in the search for the optimum pairs. At the top of the figure is plotted, to the same time scale, the smoothed power of the S-burst signal. Table 1 lists for the 10 best examples of phase coherent intervals in Figure 4 their beginning and ending times and durations, the optimum values of f_m and δ_m , and the ranges of the values of the correlation coefficient (rounded off to the second decimal place) over the indicated time intervals. The longest such interval is 115 μs , and the shortest listed in the table is 45 μs (the 25 μs interval starting at 6.37 ms, followed by a short gap and then the 78 μs interval, are considered to be a single event). As would be expected, the C -range lower limits that were closest to 1.00 were those for the phase coherent intervals at the times of strongest S-burst signal power. In Paper 1 the only observed phase coherent intervals were those between 6.75 and 6.95 ms. The others were overlooked. The conclusion stated in Paper 1 that these were the only phase coherent intervals in the entire S-burst was obviously incorrect. It now appears likely that successive intervals of phase coherence occur throughout the S-burst, but that they are more difficult to identify at times of relatively low signal strength. More observations are needed to determine if this is true.

During times at which $C(f_m, \delta_m, t) = 1$, the narrow-band of low-frequency S-burst components and the matching oscillator signal are in a condition of in-phase resonance. But when f_m is far from the S-burst frequency, the curve for $C(f_m, \delta_m, t)$ oscillates nearly sinusoidally between -1 and +1. This oscillation represents the beating of the effective S-burst frequency with the matching oscillator frequency. As the S-burst frequency drifts to progressively lower values, the beat-frequency decreases from a relatively high value to

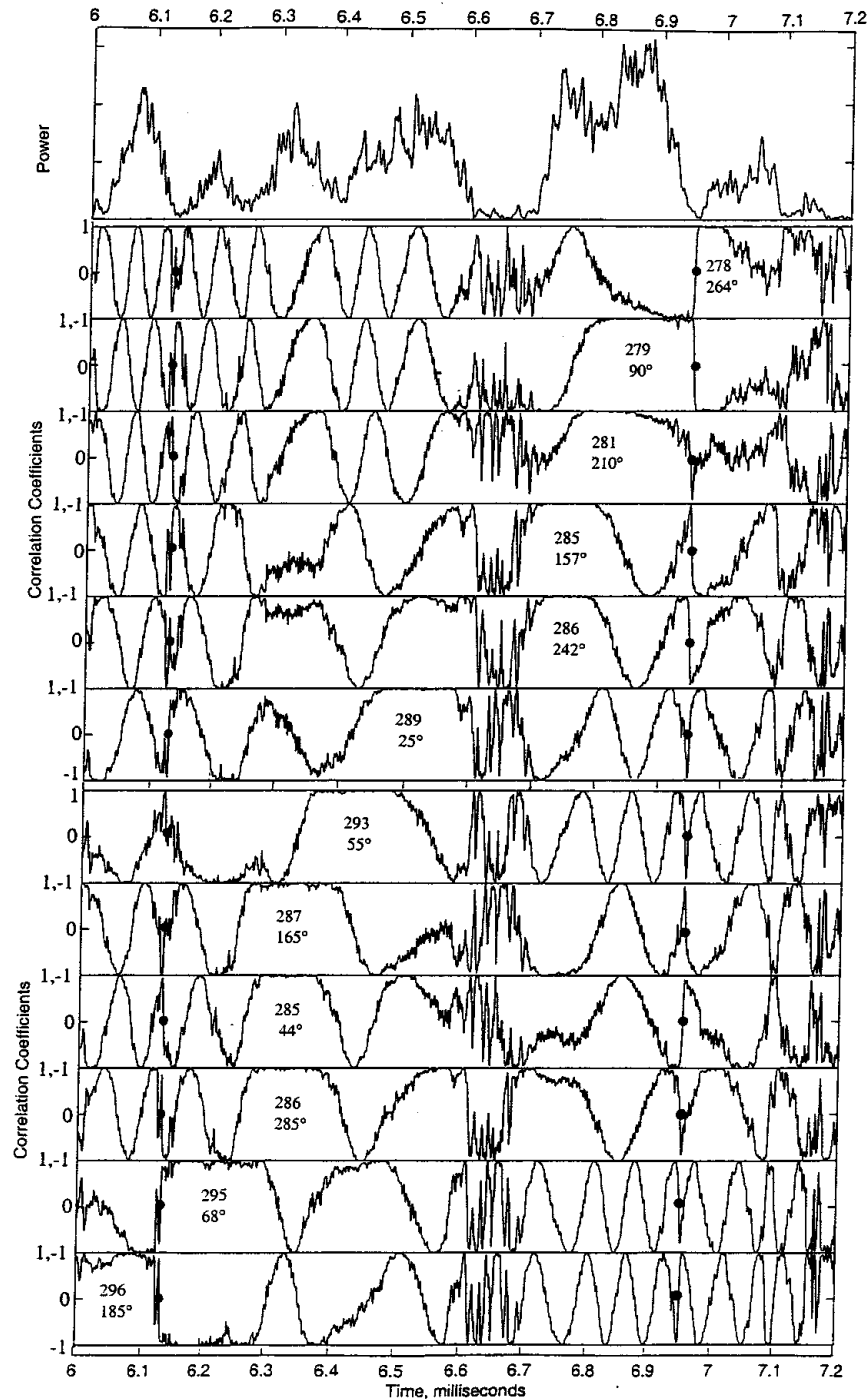


Figure 4: Top curve: S-burst power plotted versus time (the same S-burst as in Figure 3 of Paper 1). Remaining 12 curves: Plots of the correlation coefficient of the S-burst voltage with that of the matching oscillator when the latter is set to each of the pairs of frequency and phase constant values indicated under the flat-topped sections of the curves. The flat-topped sections indicate intervals of phase coherence. The two vertical columns of heavy black dots indicate times of brief drops of the S-burst intensity to zero, together with S-burst phase jumps as indicated by slope discontinuities of the correlation coefficient curves.

zero and then increases again to a high value. While the beat frequency is zero the value of $C(f_m, \delta_m, t)$ remains constant, the constants having been made equal to 1 in the phase coherent intervals displayed in Figure 4 by means of adjustments of δ_m . This explains the general appearance of the set of 12 correlation coefficient curves in the figure.

The conspicuous interval of wider-band random noise that occurs between the times 6.6 and 6.7 ms in each of the 12 curves corresponds to the times at which the S-burst signal power (in the top curve) dropped abruptly almost to zero and recovered equally abruptly after the lapse of 0.1 ms. The residual noise between 6.6 and 6.7 ms is galactic background that remains after the S-burst source has temporarily shut down.

Another interesting feature of Figure 4 is the behavior of the 12 correlation coefficient plots at the times indicated by the two vertical columns of heavy black dots (i.e., at 6.13 and 6.95 ms). These are the two times at which the power curve momentarily dropped to zero, then recovered almost immediately. It can be seen that most if not all of the 12 correlation coefficient plots exhibit phase discontinuities at these times. I associate these phase discontinuities with the termination of one episode of amplification of the S-burst wave and the starting of the next episode. Those of the phase jumps that happened to have occurred during intervals of phase coherence are most interesting. The best example is the curve for which $f_m = 279$ kHz and $\delta_m = 90^\circ$ at the time 6.95 ms. It is obvious that at this time the value of C jumped from +1 to -1, indicating a phase jump of 180° . At precisely the same time, the curve for which $f_m = 278$ kHz and $\delta_m = 264^\circ$ jumped from $C = -1$ to $C = +1$, also indicating a 180° change of phase. Several others of the curves that were exhibiting some degree of phase coherence also indicated such a phase reversal, but less conclusively so because phase coherence did not happen to be complete at the time. Similar phase slope discontinuities are also observed at the vertical column of heavy dots at $t = 6.13$ ms, although only those in the bottom two curves occurred while an interval of near-phase-coherence happened to have been in progress. The one for $f_m = 295$ kHz and $\delta_m = 68^\circ$ involved a jump from $C = -1$ to $C = +1$ while that for $f_m = 296$ kHz and $\delta_m = 185^\circ$ jumped in the opposite direction, both indicating approximately 180° phase reversals.

I tentatively suggest that the observed 180° shifts imply that the second harmonic of the observed S-burst frequency is involved in the process of maintaining phase coherence. (In general, the second harmonic becomes stronger relative to the fundamental the more relativistic are the velocities of the emitting electrons.) Let us assume that an incipient cyclotron maser co-moving with the outward stream of energetic electrons has become split so that two similar but laterally separated centers of wave amplification develop. One possible reason for the split is the presence within the 7 keV electron beam of a filamentary component consisting of electrons having energies that are too low and number densities that are too high to allow the cyclotron maser activity to extend within the region between the dual amplification centers that actually develop. The lateral separation of the two centers increases as they move outward along the diverging field lines at equal velocities. It is further assumed that one of the dual centers is emitting the observed S-burst, but the hollow-cone beam from the other is not quite aligned with Earth (perhaps because of the field line divergence). I will refer to the dual centers as the Earth-observed and the unobserved sources, respectively. Each center is amplifying the second harmonics

just above $2f_c$ in addition to the fundamental frequency components just above f_c . The local f_c values of the plasma encountered along the straight line connecting the centers are approximately equal to f_c at the centers. Wave propagation at the fundamental frequency from each center to the other will thus be impeded because of refraction of the rays in directions toward lower magnetic field intensity (i.e., away from the stop-zone boundary). In other words, each center lies outside the beam from the other. At the second harmonic frequencies, however, the beams from the two centers are relatively broad and there is no hindrance to propagation from each one to the other. Since the energetic electrons in each of the activity centers can absorb $2f_c$ radiation as well as emit it, I assume that the phase bunching needed to maintain phase coherence is provided by the second-harmonic feedback between the centers rather than by feedback at the fundamental. The second-harmonic oscillations at the two amplification centers are thus said to be *phase locked* during intervals of phase coherent emission.

Let us assume that at $t = 6.95$ ms in Figure 4 phase lock was lost due to a momentary intensity drop in the emission from the Earth-observed center and then regained after the lapse of an odd number of second-harmonic oscillations at the unobserved center. This corresponds to the same odd number of half-cycles of fundamental-frequency oscillations. The result was the abrupt phase reversal of the fundamental-frequency signal from the observed center, as indicated by the change in the correlation coefficient of the S-burst fundamental-frequency voltage with that from the matching oscillator from $C = +1$ to $C = -1$. There was a similar occurrence at $t = 6.13$ ms. It is just as probable that an even number of second-harmonic cycles as an odd number would have elapsed, in which case there would have been a phase shift of half the even number times 360° at the fundamental frequency. This is equivalent of no phase shift at all, and would not have been noticed.

Acknowledgments: The author would like to express his indebtedness to his colleagues Francisco Reyes and Wesley Greenman who have made our continuing investigation of Jovian S-burst microstructure at the University of Florida possible. Thanks are also extended to Kazumasa Imai for helpful discussions and other assistance in the preparation of this paper.

References

- Calvert, W., Y. Leblanc, and G. R. A. Ellis, Natural radio lasing at Jupiter, *Astrophys. J.*, **335**, 976–985, 1988.
- Carr, T. D., K. Imai, L. Wang, L. Garcia, F. Reyes, C. H. Higgins, and W. B. Greenman, Recent results by the University of Florida group from low frequency radio observations of Jupiter and Neptune, in *Planetary Radio Emissions IV*, edited by H. O. Rucker, S. J. Bauer, and A. Lecacheux, Austrian Academy of Sciences Press, Vienna, 25–41, 1997.
- Carr, T. D., and F. Reyes, Microstructure of Jovian decametric S-bursts, *J. Geophys. Res.*, **104**, 25127–25142, 1999.

- Flagg, R. S., and T. D. Carr, Wide bandwidth observations of the decametric bursts, from Jupiter, *Astrophys. Lett.*, **1**, 47–53, 1967.
- Flagg, R. S., W. B. Greenman, F. Reyes, and T. D. Carr, A catalog of high resolution Jovian decametric noise burst spectra, Dept. of Astronomy, Univ. of Florida Gainesville, 1991.
- Melrose, D. B., A phase–bunching mechanism for the fine structures in auroral kilometric radiation and Jovian decametric radiation, *J. Geophys. Res.*, **91**, 7970–7980, 1986a.
- Trapp, B., An analysis of the microsecond pulse structure in Jupiter’s decametric radio emission, M. Sc. thesis, Dept. of Physics and Astronomy, Univ. of Florida, Gainesville, 1971.
- Wu, C. S., and L. C. Lee, A theory of the terrestrial kilometric radiation, *Astrophys. J.*, **230**, 621–626, 1979.
- Zarka, P., T. Farges, B. P. Ryabov, M. Abada–Simon, and L. Denis, A scenario for Jovian S–bursts, *Geophys. Res. Lett.*, **23**, 125–128, 1996.